Elsevier Editorial System(tm) for Soil Dynamics and Earthquake Engineering
Manuscript Draft

Manuscript Number:

Title: SITE RESPONSE IN TECOMAN, COLIMA, MEXICO. II. DETERMINATION OF SUBSOIL STRUCTURE AND COMPARISON WITH OBSERVATIONS

Article Type: Research Paper

Keywords: subsoil exploration; seismic refraction; microtremors, SPAC method

Corresponding Author: Professor Francisco J. Chavez-Garcia, Ph.D.

Corresponding Author's Institution: Instituto de Ingeniería, UNAM

First Author: Francisco J. Chavez-Garcia, Ph.D.

Order of Authors: Francisco J. Chavez-Garcia, Ph.D.; Juan Tejeda-Jacome

Cover Letter

Dear Sir,

Please find enclose the paper SITE RESPONSE IN TECOMAN, COLIMA, MEXICO. II. DETERMINATION OF SUBSOIL STRUCTURE AND COMPARISON WITH OBSERVATIONS by J. Tejeda-Jácome and myself, which we submit for possible publication in Soil Dynamics and Earthquake Engineering. This paper is the second and final part of a two-part study of site effects in Tecoman.

Sincerely,

Francisco J. Chávez-García

Instituto de Ingeniería, UNAM

Mexico

SITE RESPONSE IN TECOMAN, COLIMA, MEXICO. II. DETERMINATION OF SUBSOIL STRUCTURE AND COMPARISON WITH OBSERVATIONS

by

Francisco J. Chávez-García[1]*, Juan Tejeda-Jácome[2]

[1]Instituto de Ingeniería, Universidad Nacional Autónoma de México, Ciudad Universitaria, Coyoacán, 04510, México D.F., Mexico, Fax +(52-55)5623.3524, email: paco@pumas.ii.unam.mx

[2]Facultad de Ingeniería Civil, Universidad de Colima

Submitted to

Soil Dynamics and Earthquake Engineering

May, 2009

* Corresponding author

ABSTRACT

In a companion paper local transfer functions were estimated at Tecoman using earthquake and microtremor data. In this paper the subsoil structure at this city is investigated using seismic refraction and cross-correlation of noise records. P- and S-wave refraction profiles were measured at five sites within the city. Standard analysis constrained only very shallow layers. The P-wave refraction deployment was also used to record ambient vibration. These data were processed using an extension of the SPAC method; cross-correlation is computed between station pairs and the results are inverted to obtain a phase velocity dispersion curve. Penetration depth was larger than that from the refraction experiments but the shear-wave velocity of the basement could not be determined. For this reason, additional microtremor measurements were made using broad band seismometers with a larger spacing between stations. The results allowed to constrain the shear-wave velocity of the basement. Site amplification computed for the final profiles compare well with observed ground motion amplification at Tecoman. The case of Tecoman illustrates that even a simple subsoil structure may require crossing data from different experiments to correctly constrain site effects.

keywords: subsoil exploration, seismic refraction, microtremors, SPAC method

1. Introduction

The relevance of site effects for ground motion prediction is well established. Ground motion amplification due to the surficial soft soils frequently conditions damage distribution during large earthquakes. We may classify approaches to site effects into two categories [1]. In the first approach, a local transfer function is estimated based usually on earthquake data. In the last 30 years, the analysis of ambient vibration with the purpose of estimating a local amplification transfer function has also gained much popularity, especially based on the use of horizontal-to-vertical spectral ratios (e.g., [2,3]). The second approach is based on numerical modeling. If we are able to determine the subsoil structure (its geometry and mechanical properties), its effect on ground motion may be computed using numerical simulation of wave propagation. Naturally, when we are able to compare empirical site effect estimates with results from numerical modeling, the reliability of the results is greatly enhanced.

In a companion paper [4] we presented a site effect study in the city of Tecoman, a small city in Mexico, located close to the northern end of the subduction zone along the Mexican Pacific coast. In that paper, local amplification due to soft soils was evaluated using both earthquake data and ambient vibration records. The comparison of the results from different types of data and different kinds of measurement instruments provided a reliable estimate of the local amplification in the city. In this paper, we present a complementary study, centered on the exploration of the subsoil structure in Tecoman. Using an exploration seismograph, we recorded refraction profiles with hammer blows as a source at five sites within the city. Both P- and S-wave refraction profiles were measured. The records we processed using standard techniques and Vp and Vs profiles were derived for each site. In addition, ambient vibration was recorded using the P-wave refraction profiles. These noise records were analysed using a recently proposed

extension of the SPAC method where a Vs profile is inverted from phase velocity dispersion curves. The results provided a reliable estimate of shallow subsoil structure under Tecoman. However, site amplification requires knowledge of both soft soil properties and basement shear-wave velocity. The small apertures used and the high frequency of the geophones precluded the determination of the structure below the soft sediments. Ambient vibration measurements, using a larger aperture array with autonomous seismographs, were necessary to completely constrain the subsoil structure. Using the complete structure, computed site effects are in good agreement with observed local amplification.

2. Data and techniques of analysis

In our companion paper [4], we introduced the city of Tecoman (Figure 1). It is located on the coastal plane, close to the Pacific coast in Mexico, where the two most recent large Mexican earthquakes have occurred [5,6]. The data analysed in this paper were recorded at Tecoman using two different types of measurements. In the first place, we used a Geometrics, 24-channel seismic refraction seismograph to explore shallow subsoil structure. 4.5 Hz vertical and horizontal geophones were used at five sites within the city (Figure 2). At each site, three different measurements were made. The first was a standard P-wave refraction test. Vertical geophone spacing and source offset were 4 m. The source was hammer blows on a steel plate placed on the ground. Five blows were stacked by the seismograph. The second experiment was an S-wave refraction profile. The spacing between horizontal geophones and the offset were decreased to 2 m. The source was lateral blows on a wooden beam, pressed to the ground by the weight of the front axis of our vehicle. Again, five blows were stacked by the seismograph. In the case of the S-

waves, we measured two profiles hitting the beam on two sides. Thus, S-wave polarity was inverted and the identification of the first arrival of shear waves in the seismograms was facilitated. Finally, we used the P-wave profile (92 m long) to record ambient vibration. At each site, five windows of 60 sec duration of ambient vibration were recorded, triggering the seismograph without a source.

The analysis of the data from the refraction seismograph was useful to constrain the shallow structure at the sites (see below). However, no information was retrieved from the underlying basement. For this reason, we also used ambient vibration records obtained using one of the arrays reported in our companion paper [4]. We used noise data recorded by six K2 accelerographs by Kinemetrics coupled to CMG40 Guralp broad band seismometers, able to record faithfully ground velocity down to 0.03 Hz. The sites where these instruments were installed are shown in Figure 2. They do not coincide with the refraction experiment sites. The latter required an open field area, whereas the K2 needed to be installed in a secured place. The six K2 recorders were manually triggered and ambient vibration was recorded simultaneously during 8 hours. We analysed these data with the extension of the SPAC method described below.

The analysis of the P- and S-wave refraction data followed standard procedures. Travel times were inverted with a least squares method to determine possible lateral variations for each profile, using the software SeisImager/2D by Geometrics. First break analysis, however, showed strong limitations. In the case of P-waves, first arrivals could only be clearly identified for distances smaller than 54 m. In the case of S waves, this distance was reduced to 28 m. Thus, only velocities of layers shallower than 20 m could be determined.

The analysis of ambient vibration obtained wither with the refraction seismograph or with the autonomous accelerographs made recourse to the SPAC method [7], using its extension to two stations [8]. This method requires that the seismic noise be stationary in time and space and

that it consists mainly of surface waves. The use of the vertical component records allows us to ascribe our results to Rayleigh waves. It has been shown [7] that the average cross-correlation between two stations, computed in the frequency domain, takes the form of a Bessel function of first class and zero order. The argument of the Bessel function is the frequency multiplied by the distance between stations and divided by the phase velocity of the surface waves. Given that the only unknown is the phase velocity, we may compute cross-correlation between station pairs using band-pass filtered noise records, and repeat that computation for many central frequencies of the filter. The resulting function may be inverted to obtain the phase velocity of Rayleigh at the central frequencies used for the band-pass filter. The method has been described in detail before [9, 10, 11]. The noise records obtained with the P-wave refraction profile described above were processed following closely [12].

During the analysis of the ambient vibration data recorded with the exploration seismograph, we tested window-lengths of different duration, from 10 to 60 sec. The shorter windows produced unreliable results for frequencies smaller than 3 Hz. Windows of 30 sec duration and larger produced stable results for frequencies larger than 2 Hz. This limit at small frequencies is the natural consequence of the small spacing between geophones (4 m) and of their 4.5 Hz eigen frequency. In fact, it is surprising that good results are obtained down to 2 Hz. At the other end, good results were obtained up to 10 Hz. Thus, ambient vibration measurements using the exploration seismograph contributed information on the shallow subsoil profile. For each site, we averaged all possible crosscorrelations at a fixed distance. For instance, the result for 4 m distance was obtained as the average of the crosscorrelation computed between all neighbouring geophones (23 station pairs for a 24 geophone profile) and for the five 60-sec recording windows. The final results were very stable.

Two-station correlation was also used to process the data recorded by the six-station, K2 array. The distances between stations are larger (between 620 m and 2.78 km) and the broad band seismometers were able to record faithfully low frequencies. Thus, this second array was able to constrain Vs velocities in the basement below the soft sediments. At the same time, the aperture of the array and the small number of stations made it impossible to identify possible lateral variations of the subsoil structure. Thus, the results from the two different measurements usefully complemented each other.

3. Results

Figure 3 shows an example of seismic section, together with the Vs 2D profile derived from the measurements at P-Torres site. The top diagram shows one of the S-wave source refraction profiles at this site. The lower diagram shows the 2D structure derived from first break measurements. Soil structure consists of essentially flat layers. It is likely that the small lateral variations in thickness are in reality a reflection of small errors in picking S-wave arrival times. The weakness of the source signal, probably coupled to the strong attenuation expected in surficial sediments, limit clear arrivals to distances less than 28 m. As a result, Vs values can be defined only for the upper 20 m. Site effects at P-Torres site were determined [4] to have a first peak at 0.68 Hz, with amplitude 7. The profile shown in Figure 3(b) has a one-way travel time of 0.055 s, implying a resonant frequency larger than 4.5 Hz. Clearly, the refraction measurements are unable to sample the sedimentary column responsible for the local amplification.

Table 1 gives the 1D profiles determined at the 5 sites where active source refraction measurements were made. The sampled thickness is small in all cases, and the Vs of the deepest

layers are small. The dominant frequencies computed for S-wave incidence on the profiles of Table 1 are larger than observed resonant frequencies at those sites [4]. The refraction experiments did not sample the soil column that governs local site effects at Tecoman, even if the explored depth is not far from 30 m. In several building codes, site effects are assigned based on average Vs for the top 30 m [13]. Our results show that this may not be adequate to correctly predict local amplification.

Consider now the results from the ambient vibration measurements using the P-wave refraction profile array. Figure 4 shows the correlation coefficients (see [7, 8], where these coefficients are defined as average crosscorrelation between station pairs normalized by the average autocorrelation) as a function of distance and frequency. For each distance, we observe the oscillations as a function of frequency that characterizes the Bessel function. The maximum values for the correlation coefficients occur at 2 Hz. For smaller frequencies, the geophones cannot record ambient vibration reliably and correlation values drop. At the other end, good results are obtained up to 10 Hz. The smaller distances are more reliable at higher frequencies. For the larger distances, correlations coefficients come from a smaller number of station pairs. The correlation coefficients were inverted to obtain a phase velocity dispersion curve at each measurement site. The results are shown in Figure 5. There are not large differences among the five sites. Shear-wave velocity at the surface is about 200 m/s at all sites. The largest phase velocities are larger than 600 m/s at 2 Hz, significantly larger than the values determined from active source refraction. The SPAC analysis of ambient vibration recorded with the P-wave refraction profile is able to see deeper in the ground than seismic refraction using hammer blows as a source due to their small energy. Hammer blows could not be well recorded by the whole geophone line. In contrast, the SPAC method is able to recover useful signal from the correlation of all station pairs, including the more distant.

The dispersion curves in Figure 5 make it clear that there is a large impedance contrast under Tecoman. However, it is not possible to identify a phase velocity for the basement below the sediments. This is clearly indicated by the results of the inversion of the phase velocity dispersion curves. The resulting model is shown in Figure 6. The velocity for the underlying half-space at each site is different as it is not constrained from the data in Figure 5. In contrast, the structure of the soft sediments is. The depth of investigation varies from site to site but is significantly larger than the depth reached with active source. However, the final layer for each model is imposed in the inversion process. Given that local amplification results from the impedance contrast between sediments and basement, the models in Figure 6 are not able to constrain site effects.

Consider now the results obtained from the application of the SPAC method to the microtremor recorded using the Guralp seismometers. These results are shown in Figure 7 for each station pair. The five plots where the correlation coefficients are zero include records at station BOMB. This station failed to lock its internal clock on the GPS signal and it had not common time with the other four. The other stations show good correlation between 0.15 and 1 Hz. On the low frequency end, correlation is lost at about 0.15 Hz for all station pairs. This was also observed in [14] and was ascribed to the limitations imposed by a temporal deployment. On the high frequency end, correlation decreases with increasing distance between stations, as expected.

The correlation coefficients shown in Figure 7 were inverted and a phase velocity dispersion curve was obtained. The result is shown in Figure 8, together with the dispersion curves determined earlier. The Guralp array constrains phase velocity in a very limited frequency range, between 0.2 and 1 Hz. It succeeds, however, in determining the phase velocity corresponding to the basement, as shown in Figure 8 by the stars tending to a fixed value of 2.7

km/s at low frequencies. There is a large gap between the phase velocities determined from the Guralp measurements and those determined from the exploration seismograph data. An intermediate size array would have been needed to fill the gap between the 92 m maximum inter station distance for the geophone deployment and 620 m, the smallest distance between Guralp seismometers.

4. Comparison between computed and observed amplification

We inverted the dispersion curves shown in Figure 8, assuming continuity between the Gurlap determined dispersion curve and those derived from the refraction seismograph data. The results are very similar to those shown in Figure 6, except that now it is possible to assign a well determined basement at the bottom of each profile. We used those profiles to compute site amplification assuming vertical incidence of S-waves. The result is shown in Figure 9. Two significant improvements are obtained relative to the site amplification that would be computed for the profiles of Table 1. The first is that the resonance frequency decreases significantly, going below 1 Hz at most of the sites, in agreement with the observations [4]. The second is that the amplitude of the amplification increases. The shear-wave velocity determined for the basement is 3 km/s, increasing the impedance contrast with the surficial layers and thereby increasing maximum amplification. The transfer functions in Figure 9 are not reliable for larger frequencies because attenuation is not included but their fundamental peaks compare reasonably well with observed amplification at those sites [4].

5. Conclusions

We have presented the results of a campaign to explore subsoil in Tecoman, Mexico. The objective was to determine the subsoil structure required to model site effects expected during future earthquakes in the region and complements a previous study which addressed estimation of local amplification. Refraction experiments were carried at five sites within the city. Both P- and S-wave profiles were measured. These data were processed using traditional first break analysis. In addition, ambient vibration was recorded using the P-wave refraction deployment and using six autonomous accelerographs, coupled to broad band sensors. Ambient vibration measurements were processed using the extension of the SPAC method to station pairs.

Refraction tests were penalized from the small power that may be transmitted to the soil by hammer blows (other sources are generally illegal, impractical or too expensive for microzonation purposes). Soft soils, which amplify the most ground motion during earthquakes, usually have small Q values, i.e., large attenuation of seismic waves. Attenuation affects most high frequency waves, those that can be generated in refraction surveys. Thus, the size of the refraction line (92 m for P-waves and 46 m for S-waves) could not be exploited and the effective length of the geophone lines was usually only half. This limited the depth for which results could be obtained to 23 m. The travel time for the resulting profiles showed that their thickness was too small to explain the dominant frequencies observed in our companion study. Thus, even if the depth of exploration reached almost 30 m and Vs30 values could have been determined, they would not have been representative of the soil deposits responsible for local site effects.

The analysis of ambient vibration records from the P-wave refraction deployment using the SPAC method produced phase velocity dispersion curves that were reliable between 2 and 10 Hz. The observed phase velocities indicated that ambient noise measurements were able to reach

larger depths than active refraction. Using ground vibration as the signal, we were able to take advantage of the whole geophone deployment because noise could be correlated even between the more distant geophone pairs. The phase velocity dispersion curves showed small differences among the five investigated sites. Those curves showed clearly that a significant impedance contrast exists at the base of the soft sediments, however, they gave no information on the shear-wave velocity of the basement. This is to be expected [1]. The large impedance contrast efficiently traps the energy within the sediments and surface waves carry little information of the basement. An additional experiment was carried out to remedy this.

We analysed ambient vibration recorded for 8 hours at six accelerographs coupled to broad band seismometers. The distances between station ranged from 620 m to 2.8 km. The results of the SPAC analysis of these data allowed us to constrain the shear-wave velocity of the basement. However, there remained a large gap between the results from these measurements and those made with the refraction seismograph. We combined the phase velocity estimates from the broad band data with those from the small refraction profiles. We believe that the 1D profiles obtained from the inversion of the combined dispersion curves are representative of subsoil ground conditions in Tecoman. A significant point is that Poisson ratios for the sediments are significantly larger than 0.25, otherwise it is impossible to obtain a good fit between observed and computed phase velocity dispersion. Poisson ratios were obtained from the refraction tests, that allowed to determine independently P and S velocities for the shallower sediments. Computed 1D transfer functions for these profiles show a good agreement with the observed site amplification reported in our companion paper [4]. The shear-wave velocity of the basement is large (3 km/s), making a large impedance contrast with the sediments and producing sizeable amplification factors (close to a factor of 10) close to those observed. When we accept that Vs30

adequately characterizes site response, we implicitly assume a Vs value of 750 m/s for the underlying basement, which is clearly too small in our case.

The case of Tecoman is somewhat surprising. In [4] it was shown that site amplification had to be carefully evaluated and that some measurements missed the fundamental resonance peak (and a higher mode could have been considered as the fundamental). We have shown that even if the soil structure is quite simple, it is not easy to estimate the properties of the basement, which are required to correctly estimate maximum amplification. The case of Tecoman illustrates that, even when subsoil structure is not complex, different data must be crossed to reliably constrain site effects.

Acknowledgments

The help of J. Cuenca, S. Cedeño, and A. Preciado was essential for the refraction measurements. M. Manakou (Aristotle University of Thessaloniki) kindly helped us with the inversion of phase velocity dispersion curves. We thank the authorities from the different schools and public buildings where the temporal seismic stations were installed. Their assistance made our measurements possible. This study was supported by CONACYT, Mexico, through the contract SEP-2003-C02-43880/A.

References

[1] Chávez-García FJ. Site effects: from observation and modelling to accounting for them in building codes. In: K.D. Pitilakis (ed.) Earthquake Geotechnical Engineering, 4th International Conference of Earthquake Geotechnical Engineering - Invited lectures, vol. 6 of the series Geotechnical, Geological and Earthquake Engineering, ISBN: 978-1-4020-5892-9, ISSN 1573-6059, DOI 10.1007/978-1-4020-5893-6, Springer, 53-72, 2007.

[2] Nakamura Y. A method for dynamic characteristics estimation of subsurface using microtremor on the ground surface. Q.R. of R.T.R.I. 1989; 30(1): 25-33.

[3] Lermo J, Chávez-García FJ (1994). Are microtremors useful in site effect evaluation?. Bull. Seism. Soc. Am. 1994; 84, 1350-1364.

[4] Chávez-García FJ, Tejeda-Jácome J. Site response in Tecoman, Colima, Mexico. I. Comparison of results from different instruments and analysis techniques. Soil Dynamics and Earthquake Engineering 2009; submitted.

[5] Pacheco J, Singh SK, Dominguez J, Hurtado A, Quintanar L, Jiménez Z, Yamamoto J, Gutierrez C, Santoyo M, Bandy W, Guzmán M, Kostoglodov V, Reyes G, Ramirez C. The October 9, 1995 Colima-Jalisco, México earthquake (MW 8): an aftershock study and a comparison of this earthquake with those of 1932. Geophys, Res. Lett. 1997; 24: 2223-2226.

[6] Singh SK, Pacheco JF, Alcántara L, Reyes G, Ordaz M, Iglesias A, Alcocer SM, Gutiérrez C, Valdés C, Kostoglodov V, Reyes C, Mikumo T, Quaas R, Anderson JG. A preliminary report on the Tecomán, Mexico earthquake of 22 January 2003 (Mw 7.4) and its effects. Seism. Res. Lett. 2003; 74: 279-289.

[7] Aki K. Space and time spectra of stationary stochastic waves, with special reference to microtremors. Bull. Earthquake Res. Inst. Tokyo Univ. 1957; 25: 415–457.

[8] Chávez-García FJ, Rodríguez M, Stephenson WR. An alternative approach to the SPAC analysis of microtremors: exploiting stationarity of noise. Bull. Seism. Soc. Am. 2005; 95: 277-293.

[9] Metaxian JP. Etude sismologique et gravimétrique d'un volcan actif: Dynamisme interne et structure de la Caldeira Masaya, Nicaragua, Ph.D. Thesis, Université de Savoie, 319 pp. (in French), 1994.

[10] Chouet BC, DeLuca G, Milana P, Dawson M, Martín C, Scarpa R. Shallow velocity structure of Stromboli volcano, Italy, derived from small-aperture array measurements of Strombolian tremor. Bull. Seism. Soc. Am. 1998; 88: 653–666.

[11] Ferrazzini V, Aki K, Chouet B. Characteristics of seismic waves composing Hawaiian volcanic tremor and gas-piston events observed by a near-source array. J. Geophys. Res. 1991; 96: 6199–6209.

[12] Chávez-García FJ, Rodríguez M, Stephenson WR. Subsoil structure using SPAC measurements along a line. Bull. Seism. Soc. Am. 2006; 96: 729-736.

[13] Borcherdt RD. Estimates of site-dependent response spectra for design (methodology and justification). Earthq. Spectra 1994; 10: 617–653.

[14] Chávez-García FJ, Rodríguez M. The correlation of microtremors: empirical limits and relations between results in frequency and time domains. Geophys. J. Int. 2007; 171: 657-664.

Figure captions

Figure 1. Location map of Colima and Tecoman in Mexico. Subduction zone is shown as the solid line, parallel to the coast, with the solid triangles. The solid rectangle shows the location of Tecoman city. The solid triangle indicates the location of Colima's volcanoe.

Figure 2. Location of the five sites in Tecoman where refraction measurements were made (open stars). Also shows are the six sites where ambient vibration was measured using broad band seismometers (solid circles).

Figure 3. (a) An example of the S-wave refraction seismic section recorded at Tecoman. The records shown correspond to P-Torres site. (b) 2D S-wave subsoil structure derived from the inversion of first break S-wave arrivals at P-Torres site. Velocity values are given in m/s.

Figure 4. Correlation coefficients as a function of frequency and distance computed from ambient noise measurements using the P-wave refraction deployment at BOMB site. The result at a given distance was obtained as the average of all possible geophone pairs at that distance. These results correspond to the average for five 60 sec recorded windows.

Figure 5. Phase velocity dispersion curves obtained from the correlation coefficients computed from ambient noise measurements using the P-wave refraction deployment at each of the five sites where refraction measurements were made. Shear-wave velocities attain values larger than 600 m/s.

Figure 6. Shear-wave velocity profiles determined from the inversion of the dispersion curves shown in the previous figure.

Figure 7. Correlation coefficients from ambient vibration recorded with the six station array of accelerographs coupled to broad band seismometers. Each diagram corresponds to a station pair separated the distance (in km) indicated. The five diagrams which show zero correlation correspond to correlation using records at site BOMB, which did not have a common time base with the other five instruments.

Figure 8. Final phase velocity dispersion curves obtained for Tecoman. The dispersion curves shown in Figure 5 are plotted together with the dispersion curve derived from the inversion of the correlation coefficients computed for the Guralp array.

Figure 9. Computed soil amplification for vertical incidence of S-waves on the five soil profiles determined at Tecoman from the inversion of phase velocity dispersion shown in the previous figure.

Table 1. Soil profiles obtained from first-break analysis of the refraction tests

Thickness [m]	S-wave velocity [m/s]	P-wave velocity [m/s]
P-Torres		
3.0	279	505
4.0	363	660
12.0	403	740
BOMB		
0.8	90	204
5.7	220	205
6.5	283	510
C-VERDE		
4.0	256	466
8.5	377	698
2.5	450	846
S-HELENA		
4.0	258	595
9.0	334	790
3.0	483	920
UDEP		
3.0	300	570
7.0	338	660
11.0	404	750

Figure1

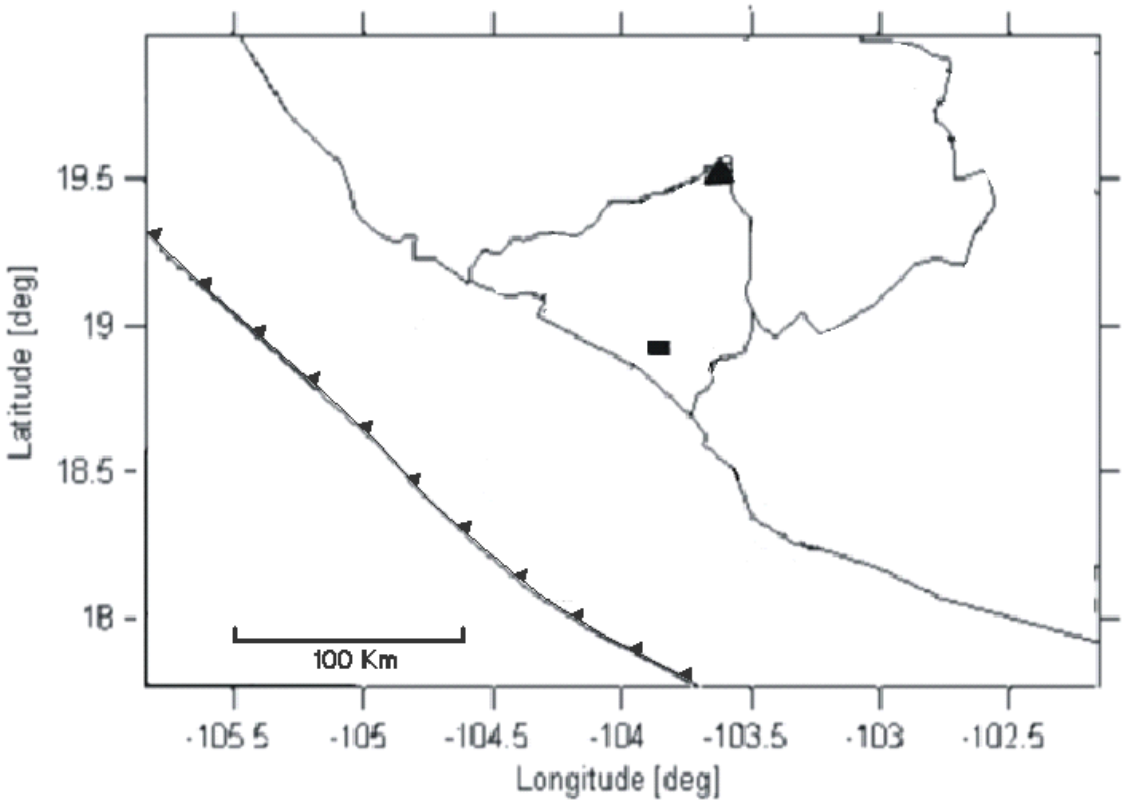
19.5
19
18.5
18
Latitude [deg]
100 Km
-105.5
-105
-104.5
-104
-103.5
-103
-102.5
Longitude [deg]

Figure2

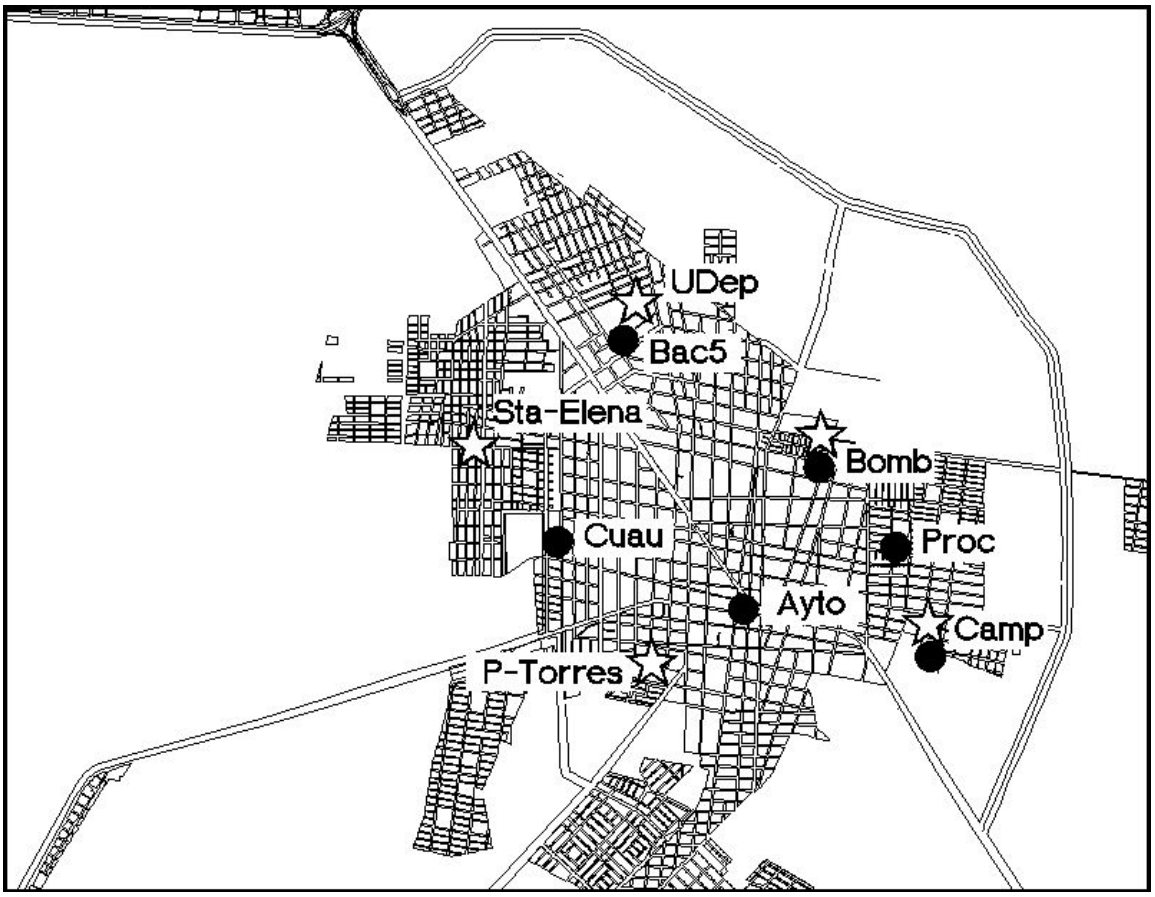

Figure3

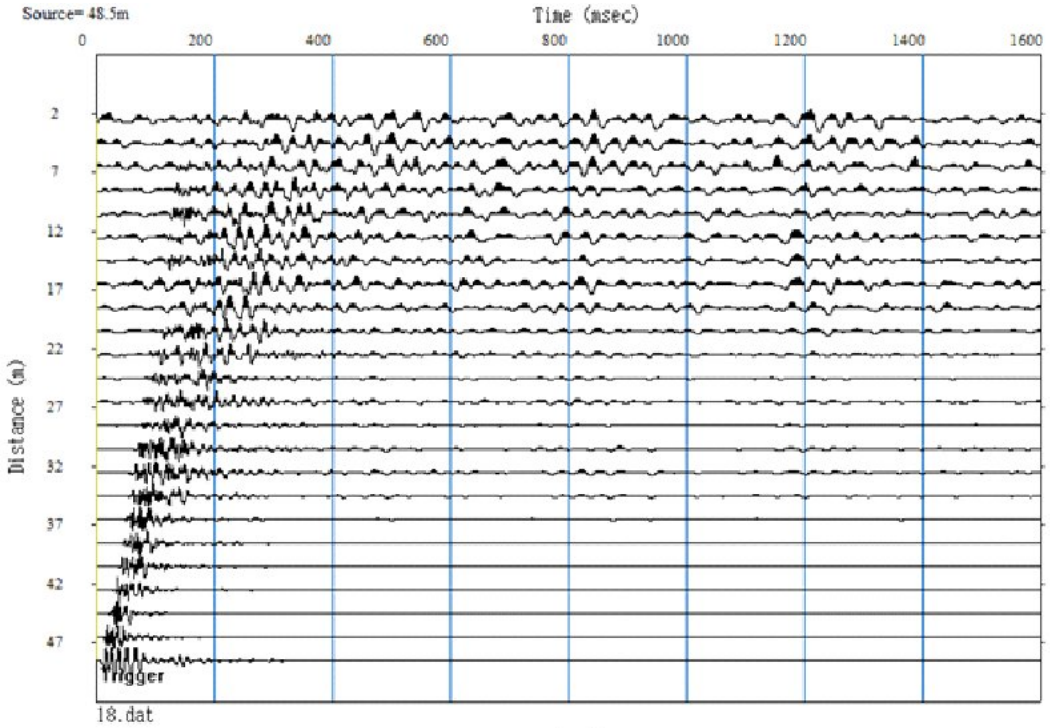
Source= 48.5m
Time (msec)
0
200
400
600
800
1000
1200
1400
1600
Distance (m)
2
7
12
17
22
27
32
37
42
47
Trigger
18.dat

(a)

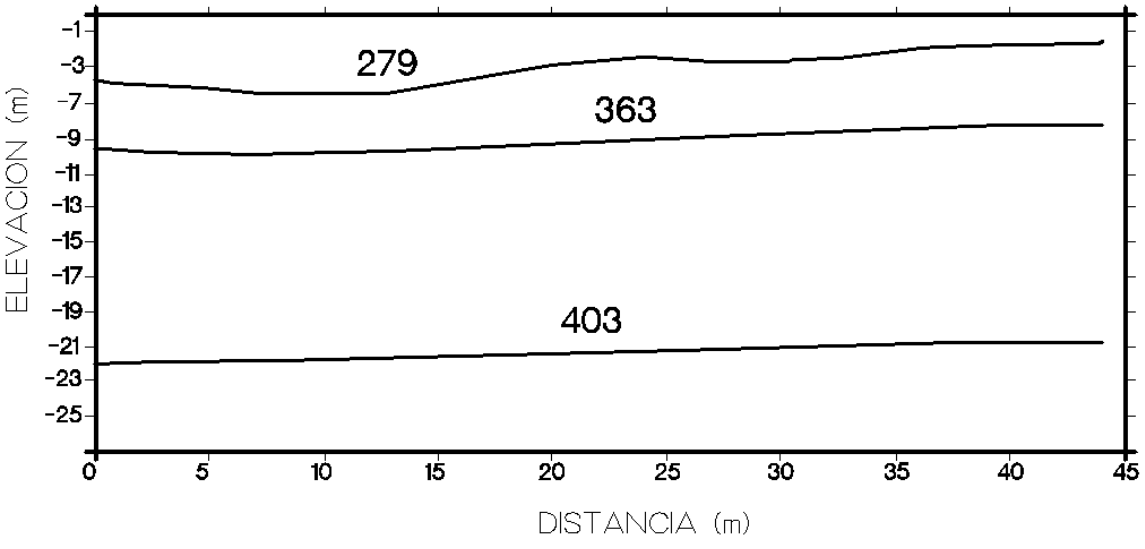
ELEVACION (m)
-1
-3
-7
-9
-11
-13
-15
-17
-19
-21
-23
-25
279
363
403
0
5
10
15
20
25
30
35
40
45
DISTANCIA (m)

(b)

Figure4

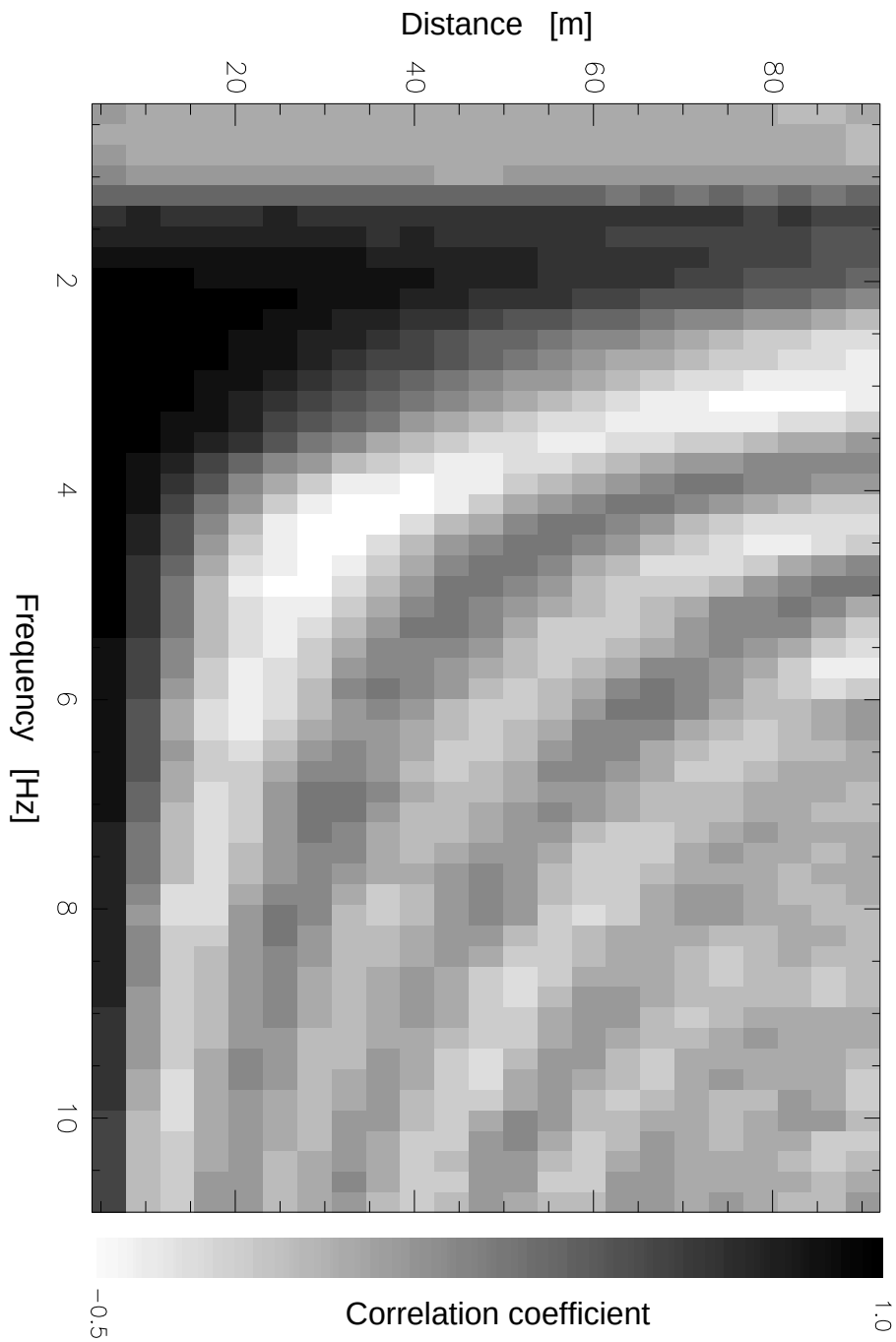
Distance [m]
20
40
60
80
Frequency [Hz]
2
4
6
8
10
Correlation coefficient
−0.5
1.0

Figure5

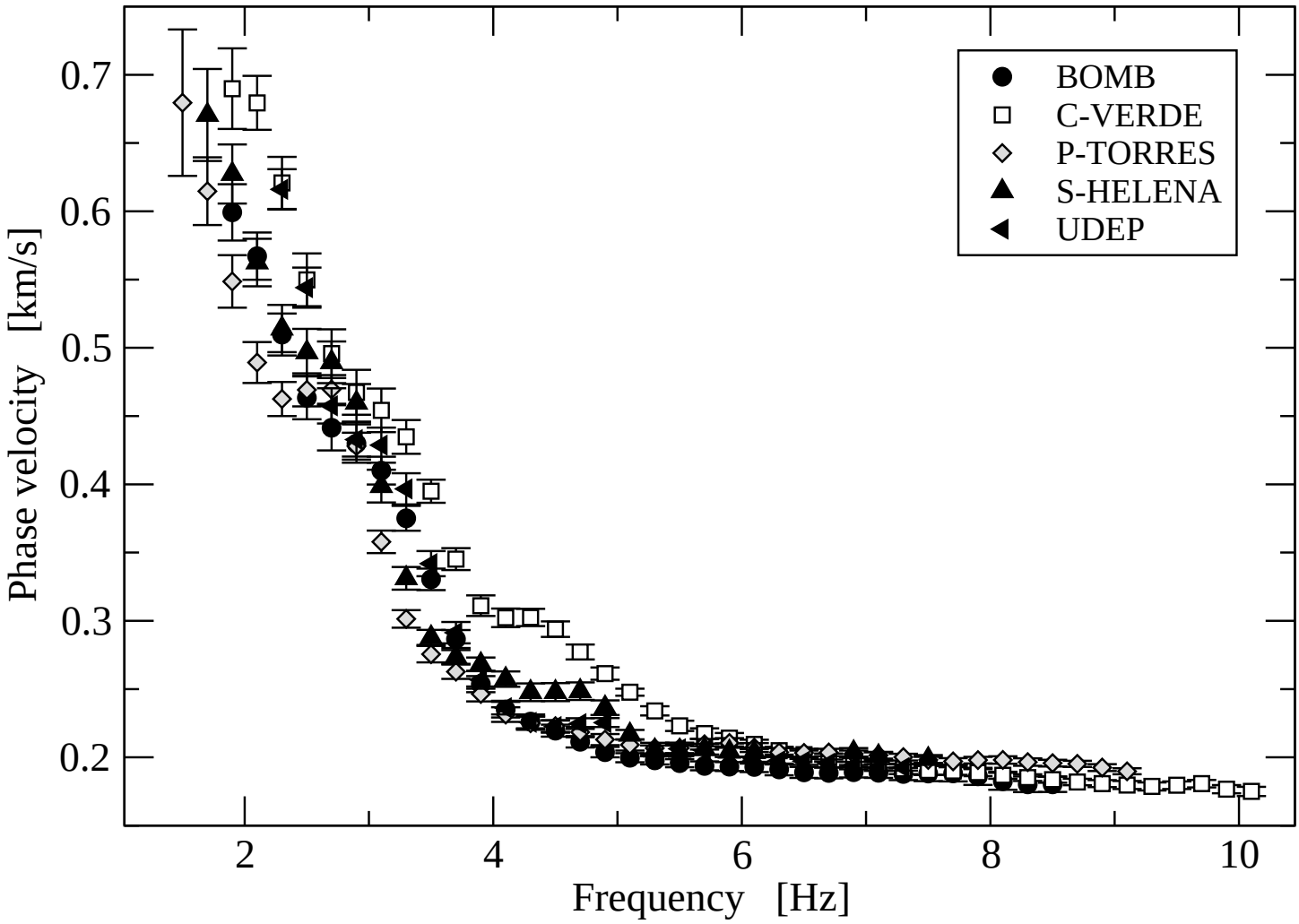
BOMB
C-VERDE
P-TORRES
S-HELENA
UDEP
Phase velocity [km/s]
Frequency [Hz]
0.2
0.3
0.4
0.5
0.6
0.7
2
4
6
8
10

Figure6

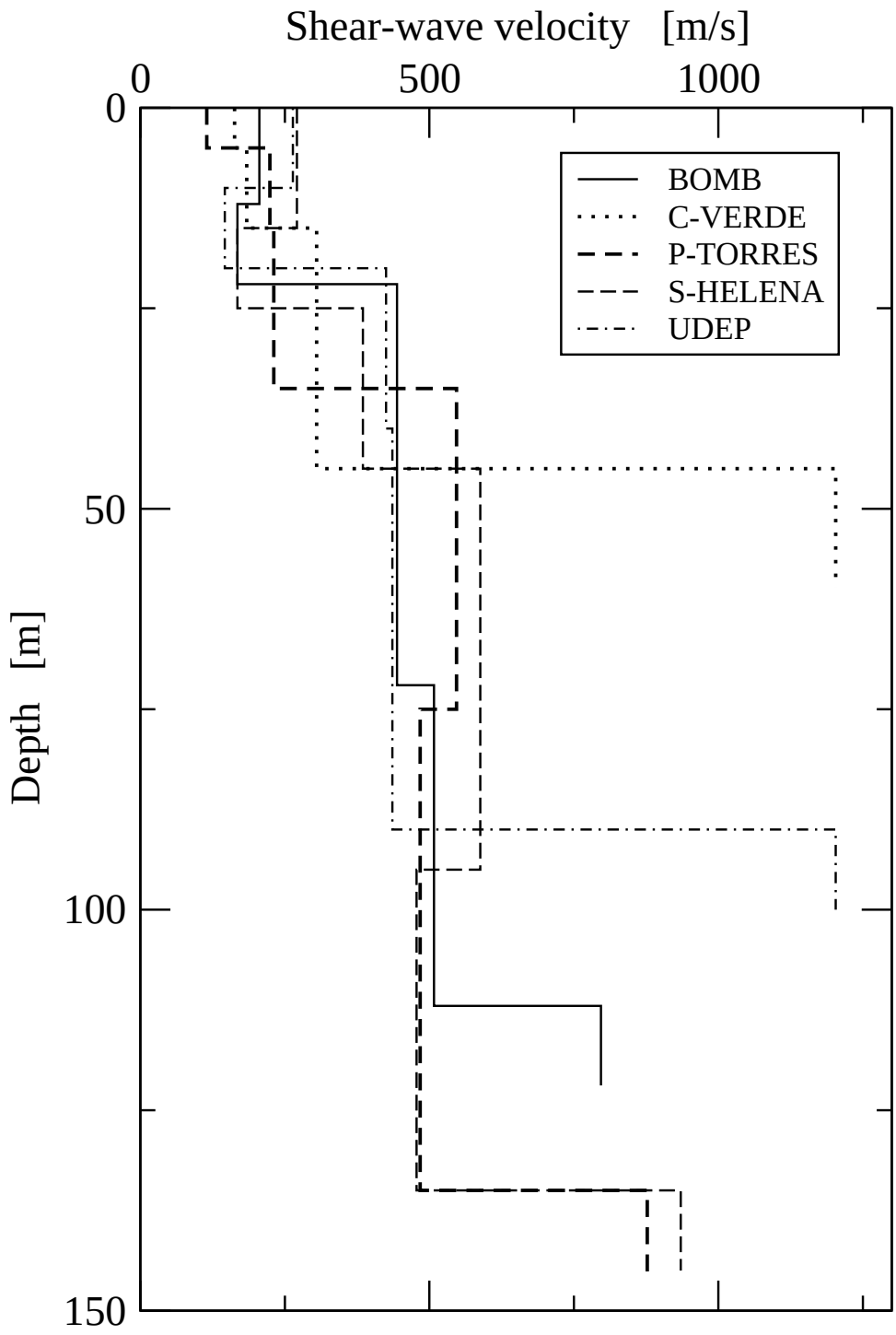
Shear-wave velocity [m/s]
0
500
1000
0
50
100
150
Depth [m]
BOMB
C-VERDE
P-TORRES
S-HELENA
UDEP

Figure7

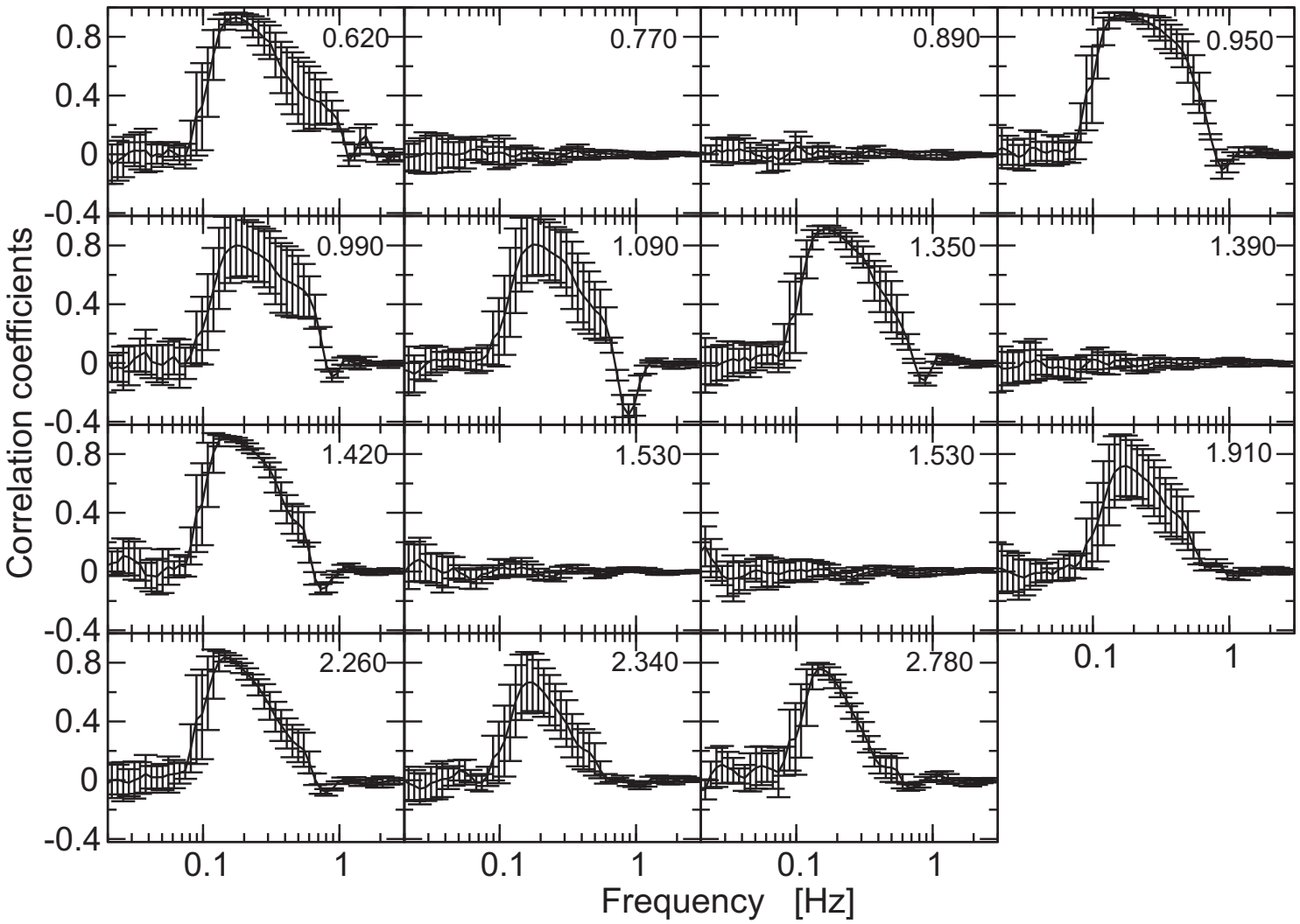
0.620
0.770
0.890
0.950
0.990
1.090
1.350
1.390
1.420
1.530
1.530
1.910
2.260
2.340
2.780
0.8
0.4
0
-0.4
0.1
1
Correlation coefficients
Frequency [Hz]

Figure8

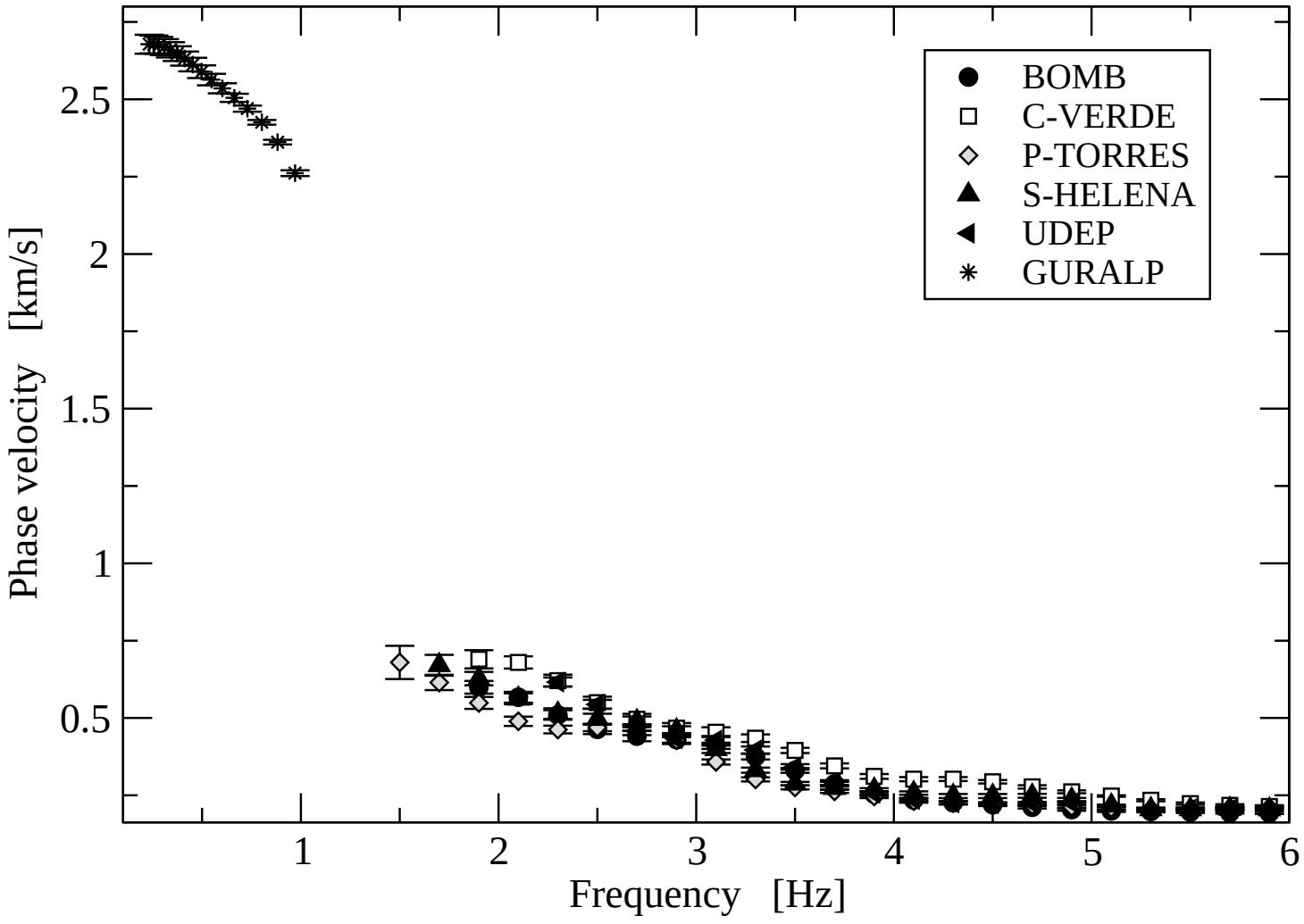
BOMB
C-VERDE
P-TORRES
S-HELENA
UDEP
GURALP
Phase velocity [km/s]
Frequency [Hz]
0.5
1
1.5
2
2.5
1
2
3
4
5
6

Figure9

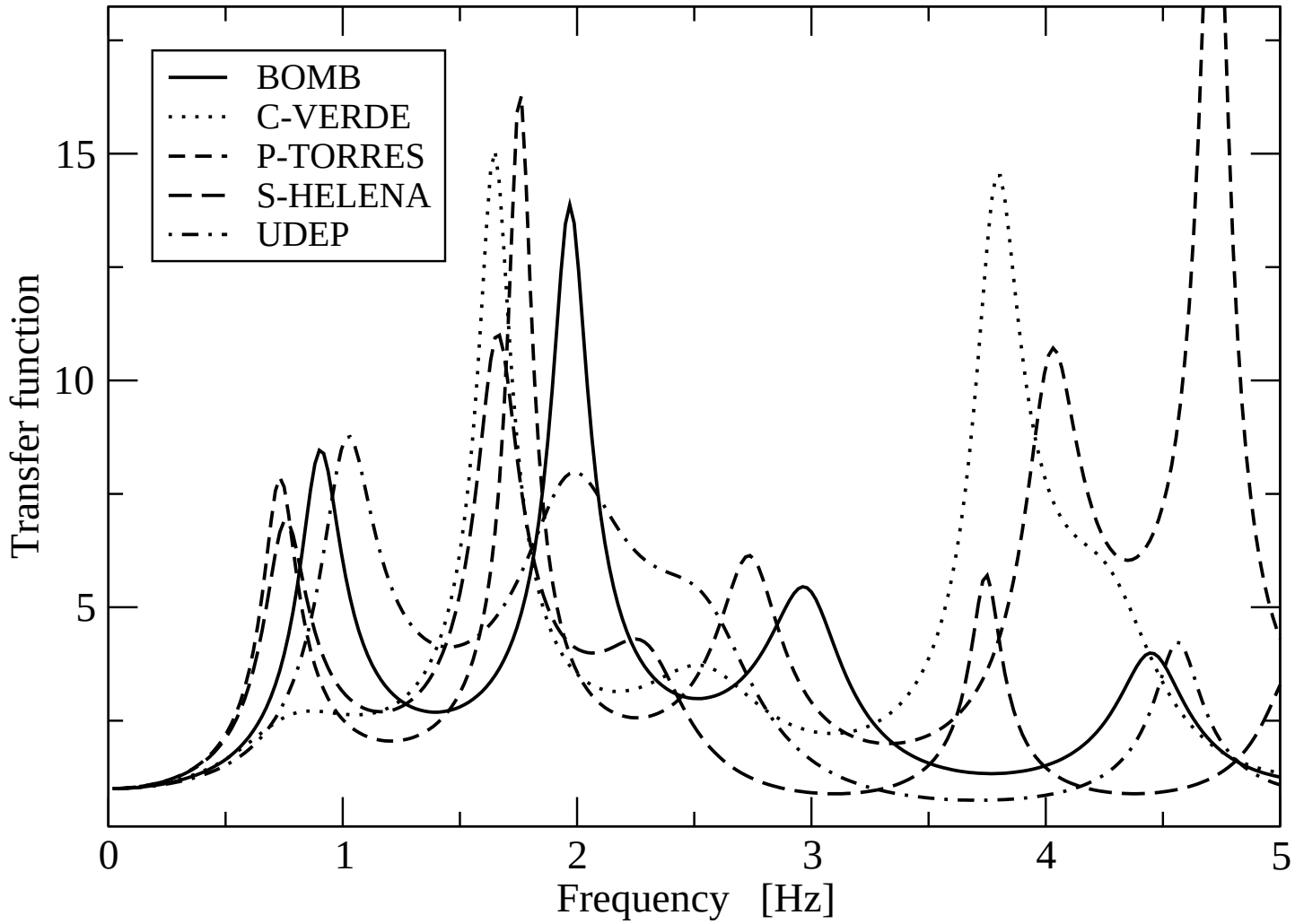
BOMB
C-VERDE
P-TORRES
S-HELENA
UDEP
Transfer function
15
10
5
0
1
2
3
4
5
Frequency [Hz]